ELSEVIER

Catalysis Today 45 (1998) 191–196

CATALYSIS TODAY

Production of carbon monoxide and hydrogen by methanol decomposition over nickel dispersed on porous glass

Yasuyuki Matsumura*, Koji Kuraoka, Tetsuo Yazawa, Masatake Haruta

Osaka National Research Institute, AIST, Ikeda, Osaka 563, Japan

Abstract

The methanol decomposition to carbon monoxide and hydrogen is catalyzed at 200°C over nickel supported on porous glasses of which major pore diameters are 4, 19, and 45 nm. The catalyst in which the crystallite size of nickel is close to the pore diameter of 19 nm is the most active while in other samples the crystallite size is significantly different from the pore diameter, suggesting that the reaction over nickel particles is enhanced in the pore of which size is close to that of the particles.

Keywords: Nickel supported on silica; Methanol decomposition; Pore size; Particle size of nickel

1. Introduction

Methanol, which can be synthesized from most of carbon resources via syn-gas, is a possible energy carrier because the transportation and storage are easy [1,2]. It is often beneficial that the on-site reforming of methanol to hydrogen and carbon monoxide increases the heating value of the fuel [3]. Nickel supported on silica is a fairly active catalyst for this endothermic reaction [4–7]. The metal particles are usually dispersed on the porous support to improve the catalytic activity, however, it is not clear whether the metal particles are located in the pore or on the external surface. Since adsorption of chemical compounds such as alcohol takes place on the surface of silica on which silanol groups are present [8–12], the concentration of the reactants in the pore is expected to be higher than on the external surface. Hence, the size and structure of the pores would affect the catalytic activity of the metal particles as well as chemical interaction between the metal and its support.

In this report, we employed porous glass with a considerably narrow distribution of pore size as a support of nickel and has studied the relationship between the catalytic activity in the decomposition of methanol and the location of nickel particles on the support.

2. Experimental

Three porous glasses whose major pore sizes were ca. 4, 19, and 45 nm (denoted as G[4], G[19] and G[45], respectively) were synthesized according to the method reported in Ref. [13]. The samples were comprised of SiO_2, B_2O_3, and Na_2O and the contents of B and Na were listed in Table 1. Silica (SiO_2) was obtained from a commercial source (Fuji-Silicia, ID-G). These samples were impregnated with nickel

*Corresponding author. Tel.: +81-727-51-9652; fax: +81-727-51-9629.

0920-5861/98/$ – see front matter
PII: S0920-5861(98)00214-4

Table 1
Chemical analyses for the supports

Support	Content (%)	
	B	Na
G[4]	1.2	0.11
G[19]	1.5	0.04
G[45]	<0.01	0.004

nitrate (GR grade, Kanto Chemicals) by evaporation of the aqueous solution at 80°C. After drying in air at 120°C, they were heated in air at 500°C for 5 h mainly for removal of NO_3^- anions. The samples contained 10 wt% of nickel (Ni/G[4], Ni/G[19], Ni/G[45], and Ni/SiO_2) except 2 wt%Ni/G[4] containing 2 wt% of nickel.

The catalytic experiments were performed in a fixed-bed continuous flow reactor operated under atmospheric pressure. The catalyst was sandwiched with quartz wool plugs in a tube reactor made of stainless steel whose contribution to the reaction was negligible. After reduction of the sample (0.5 g) in a flow of hydrogen diluted with argon (H_2, 1.8 $dm^3\ h^{-1}$; Ar, 9.0 $dm^3\ h^{-1}$), the catalyst was kept at 200°C under an argon stream (9.0 $dm^3\ h^{-1}$); then, 3.0 $dm^3\ h^{-1}$ of methanol gas was added to the flow. The reactant and products were analyzed with an on-stream Ohkura 802 gas chromatograph equipped with a TC detector. Two columns, one activated carbon (2 m, Ar carrier) and the other Porapak T (2 m, He carrier), were employed in the analyses.

Adsorption experiments were performed in a vacuum system equipped with a Baratron pressure gauge at room temperature. Just before the adsorption of hydrogen, a fresh sample was reduced with hydrogen (20 kPa) at 500°C for 1 h and evacuated at the same temperature for 0.5 h.

Distribution of pore diameter of the samples was determined from the adsorption and desorption isotherm of nitrogen obtained with a BELSORP 28 (BEL Japan) except G[45] and Ni/G[45] for which mercury porosimetry with a Micromeritics PORESIZER 9310 was adopted.

Powder X-ray diffraction (XRD) patterns for the catalysts after the reaction were recorded with a Rigaku Rotaflex 20 diffractometer using nickel-filtered CuK_α radiation in the range of 3–60° in 2θ. The mean crystallite size of nickel in a sample was determined from the width of the peak at 44.3° [Ni(111)] using the equation of Sherrer [14].

Surface analyses by XPS were carried out using a Shimadzu ESCA 750. The sample taken out from the reactor after the reaction was mounted on a sample holder in air and set into the spectrometer. Argon-ion sputtering of the sample was carried out (2 kV, 0.5 min) just before the measurement mainly for removal of oxygen adsorbed on the sample. The XPS data were calibrated by assuming that the binding energy of the C 1s peak is 284.6 eV.

3. Results

3.1. Methanol decomposition

The decomposition of methanol to carbon monoxide and hydrogen was selectively catalyzed over the nickel catalysts at 200°C. The methanol conversion was the highest with Ni/G[19] and the activity of Ni/SiO_2 was fairly low (Table 2).

Table 2
Catalytic activity of nickel supported on porous glass for the methanol decomposition to hydrogen and carbon monoxide at 200°C and hydrogen adsorption on the catalyst

Catalyst	Methanol conversion	Adsorption parameters for H_2[a]			Surface area of nickel	Crystallite size of nickel (nm)	
		v_0	v_1	K		H_2 adsorption	XRD
	(%)	(μmol g^{-1})	(μmol g^{-1})	(kPa)	(m^2 g-cat^{-1})		
Ni/G[4]	7.5	21	37	0.34	4.4	12	10
Ni/G[19]	8.4	16	21	0.53	2.8	19	16
Ni/G[45]	2.7	1	31	0.42	2.4	23	22
Ni/SiO_2	5.6	8	35	0.47	3.3	17	15
2 wt%Ni/G[4]	3.5	6	12	0.32	1.3	8	7

[a] $v = v_0 + v_1 K^{1/2} P_{H_2}^{1/2} / (1 + K^{1/2} P_{H_2}^{1/2})$, where v is amount of hydrogen adsorbed and P_{H_2} is a partial pressure of hydrogen.

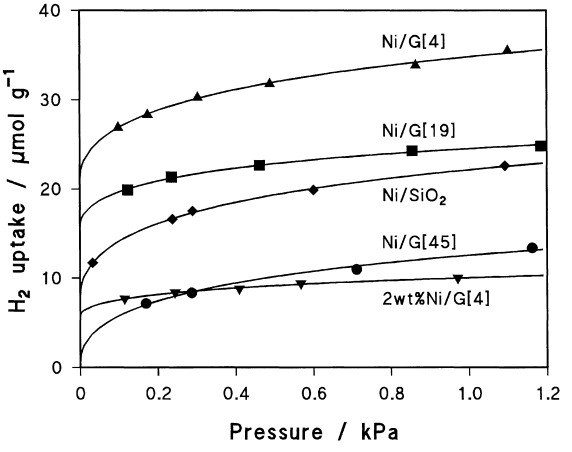

Fig. 1. Adsorption isotherms for hydrogen on nickel supported on porous glass.

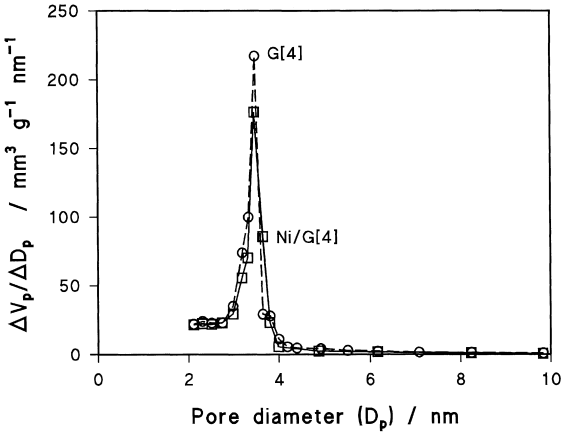

Fig. 2. Pore distributions for G[4] and Ni/G[4]. D_p, pore diameter; V_p, pore volume.

3.2. Adsorption of hydrogen

Adsorption of hydrogen on the nickel samples was carried out at room temperature after reducing treatment with hydrogen at 500°C (Fig. 1). The adsorption isotherms were fit with an equation of $v = v_0 + v_1 K^{1/2} P_{H_2}^{1/2} / (1 + K^{1/2} P_{H_2}^{1/2})$ where v is hydrogen uptake and P_{H_2} is pressure of hydrogen. The curves in Fig. 1 were drawn using the equation and the constants were given in Table 2.

3.3. Physical properties of the catalysts

In the XRD patterns for the nickel catalysts, only the peaks at 44.3° [Ni(111)] and 51.7° [Ni(200)] in 2θ were present except the broad peak for silica [15]. The crystallite sizes of nickel metal were 7–22 nm determined from the width of the strong peak at 44.3° (see Table 2).

The distribution of pore diameter in Ni/G[4] was almost the same as that in G[4] (Fig. 2). However, the distributions for Ni/G[19] and Ni/G[45] were different from those for the supports (Figs. 3 and 4). The distribution for Ni/SiO_2 was similar to that for the original support (Fig. 5). The BET surface areas for the catalysts were smaller than those for the original solids (Table 3). The pore volumes were also reduced after impregnation with nickel.

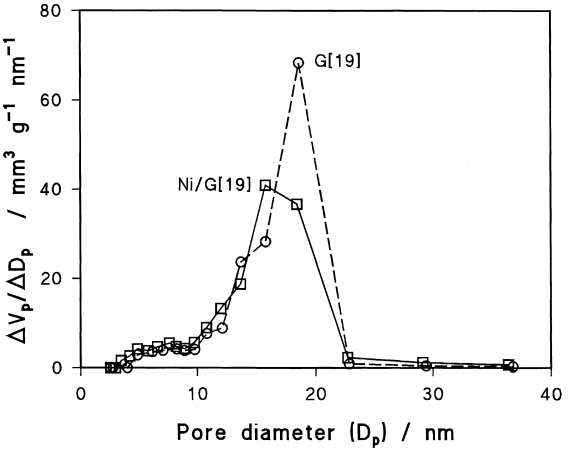

Fig. 3. Pore distributions for G[19] and Ni/G[19].

3.4. Surface analyses by XPS

The surface analyses by XPS were carried out with the nickel catalysts just after taken out from the reactor. The binding energies recorded were 853.2±0.2 eV for Ni $2p_{3/2}$, 103.2±0.2 eV for Si 1s, and 532.8±0.1 eV for O 1s regardless of the samples. The surface atomic ratio of Ni/Si was determined from the peak areas using atomic sensitivity factors (3.0 for Ni $2p_{3/2}$, and 0.27 for Si 1s) [16]. The value for Ni/G[4] was 0.21, significantly higher than the other samples (Table 4). After ground to fine powder, the sample was analyzed again and the value was reduced

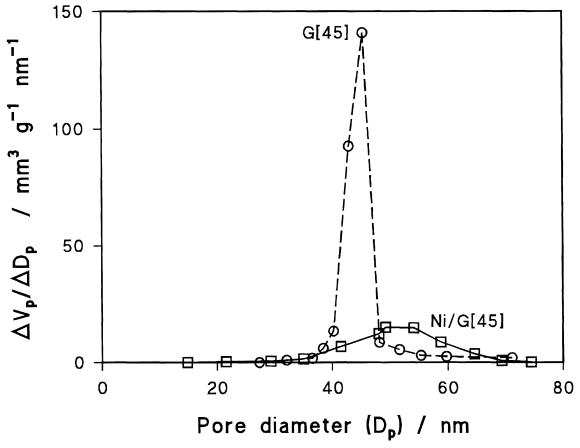

Fig. 4. Pore distributions for G[45] and Ni/G[45].

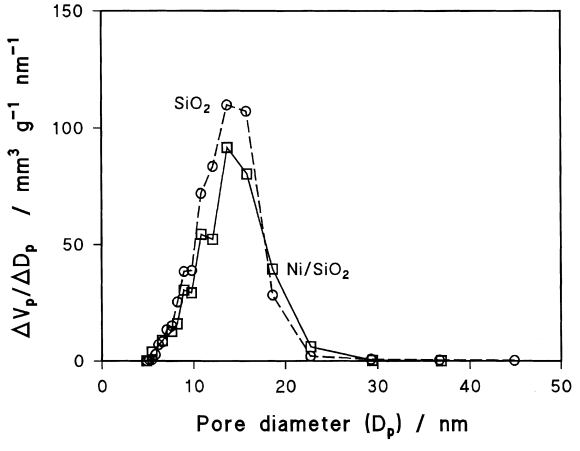

Fig. 5. Pore distributions for SiO_2 and Ni/SiO_2.

to 0.08. On the contrary, the ratio for Ni/G[45] was 0.03 while the value was appreciably increased to 0.05 after grinding.

4. Discussion

It is known that one hydrogen atom is stoichiometrically adsorbed on a nickel atom site [15], hence, the number of nickel atoms exposed on surface can be determined from the amount of hydrogen adsorbed at saturation (v_0+v_1). The parameter, K, is the equilibrium constant for weak adsorption of hydrogen on nickel surface while the values obtained (see Table 2) are fairly close. The surface area of nickel (S_{Ni}) can be calculated assuming the cross section of a nickel atom as 0.0633 nm^2 [17]. The mean crystallite size (D) is calculated using an equation of $D=54.3/S_{Ni}$ expressing D in nm and S_{Ni} in m^2 g-cat^{-1}, employing a full sphere crystalline model [17]. The diameters calculated are close to those from the XRD data (see Table 2), appearing that the estimation of the number of nickel atoms exposed on the surface is appropriate.

After impregnation of nickel the pore distribution and the surface area of G[45] were dissimilar to the original support (see Fig. 4 and Table 3). In the process of impregnation metal particles often plug narrow pores of a porous support (choking). However, the diameter of pores in both the original and impregnated samples are considerably larger than the crystallite size of nickel whose total volume in the sample is only 11 mm^3 g-cat^{-1}. Thus, the dissimilarity in the pore distribution and surface area are not mainly caused by choking of pores with nickel particles but may be due to shrink of the structure during calcination and/or reduction of the sample. The mean surface atomic ratio of Ni/Si can be calculated from the number of surface nickel determined by hydrogen adsorption and from the surface area for the part of SiO_2 in Ni/G[45], assuming that the cross sections of an SiO_2 molecule and an Ni atom are 0.113 and 0.0633 nm^2, respectively. The ratio calculated is 0.20 and considerably higher than the Ni/Si ratio (0.03) determined by the

Table 3
Surface areas and pore volumes of the catalyst and its support

Catalyst	BET surface area (m^2 g^{-1})		Surface area (m^2 g^{-1})		Pore volume (mm^3 g^{-1})		Diameter of major pore (nm)	
	Support	Catalyst	Support	Catalyst	Support	Catalyst	Support	Catalyst
Ni/G[4]	162	111	133	122	114	104	3.7	3.5
Ni/G[19]	87	77	101	93	407	342	18.6	15.8
Ni/G[45]	57	23	67	24	751	294	45.4	49.2
Ni/SiO_2	176	153	266	221	889	762	13.7	13.7

Table 4
Surface properties of the nickel catalysts

Catalyst	Ni/Si atomic ratio		Number of Ni atoms exposed (μmol g-cat^{-1})	TOF[c] (h^{-1})
	XPS[a]	Adsorption[b]		
Ni/G[4]	0.21	0.07	117	172
Ni/G[19]	0.09	0.07	73	307
Ni/G[45]	0.03	0.20	62	117
Ni/SiO_2	0.01	0.04	86	174
2 wt%Ni/G[4]	0.02	0.01	35	267

[a]Surface atomic ratio determined by XPS.
[b]Surface atomic ratio estimated from the number of nickel atom and BET surface area.
[c]Turn-over frequency calculated from the number of nickel sites and the methanol conversion.

XPS analyses which mainly give information on the external surface of the sample (Table 4), appearing that nickel particles dominantly locate on the surface of the pores. This is also evidenced by the increase in the Ni/Si ratio obtained after grinding the sample to fine powder.

On the contrary, the Ni/Si ratio for Ni/G[4] is considerably higher than that after grinding. The ratio of Ni/Si determined from the surface areas for this sample is 0.07 and significantly lower than that from XPS, showing that nickel particles distribute mainly on the external surface of the support. It is also evidenced by the crystallite size of nickel estimated from both the XRD measurement and the hydrogen adsorption (see Table 2), which is apparently larger than the pore diameter of the support. The BET surface area of G[4] is considerably larger than the surface area calculated from the pore distribution assuming cylindrical pores (see Table 3). This suggests presence of small pores whose pore diameter is less than 2 nm in G[4] while the major part of the small pores are probably chocked by nickel particles after the impregnation.

The crystallite size of nickel on Ni/G[19] is close to the pore diameter of the sample (cf. Fig. 3 and Table 2). Since the atomic ratio determined by XPS is also close to that from the adsorption results (see Table 4), the nickel particles are rather homogeneously distributed both on the external surface and the pores. The nickel particles do not seriously choke the pores because the surface area or the pore volume of the support was not significantly reduced by the impregnation of nickel. The change in the distribution of pore diameter after the impregnation of nickel could be caused by partial destruction of the pore structure during the calcination at 500°C.

The distribution of pore diameter for Ni/SiO_2 is similar to Ni/G[19] while the surface area and the pore volume for the former sample are significantly larger than those for the latter. The mean crystallite size of nickel estimated from XRD and hydrogen adsorption is in the range of the size for the larger pores in Ni/SiO_2 (cf. Table 2 and Fig. 5). It should be noted that the surface area calculated on the basis of the pore distribution is significantly larger than the BET surface area. Since the former surface area is calculated from the size and volume of pores assuming cylindrical pores, the larger area suggests that the pore is in the shape of bottle and the size calculated is that at the bottle neck. The mean pore diameter can be calculated from the BET surface area and the pore volume assuming that pores are cylindrical and uniform. The value for Ni/SiO_2 is 19.9 nm which is appreciably larger than the crystallite size of nickel (see Table 2) while those for Ni/G[4], Ni/G[19], and Ni[45] are 3.7, 17.8, and 51.1 nm. The surface atomic ratio of Ni/Si determined by XPS is small, appearing that nickel particles are mainly present in the pores.

The turn-over frequencies (TOFs) of nickel sites on the catalysts for the methanol decomposition can be calculated from the methanol conversion and the number of nickel sites obtained from the adsorption isotherms of hydrogen (see Table 4). The lowest TOF is produced with Ni/G[45] in which fairly large nickel crystallites are present. However, the crystallite size of nickel does not simply relate to the value of TOF, e.g. Ni/G[4] does not produce the highest TOF while the

crystallite size is the smallest in the catalysts containing 10 wt% of nickel (see Tables 2 and 4).

The TOF is the highest with Ni/G[19] in which the crystallite size of nickel is close to the pore diameter. On the other hand, the crystallite size is significantly smaller than the pore diameter in Ni/G[45] whose TOF is the smallest. It can be supposed that interaction between methanol and surface of glass, on which silanol groups are present, results in increase in concentration of methanol around nickel crystallites when the pore size is close to the size of the nickel crystallites. In the case of Ni/G[4] the TOF value is higher than that for Ni/G[19] although the major part of nickel particles on the former catalyst are believed on the external surface. The value for 2 wt%Ni/G[4] is close to that for Ni/G[19] while the Ni/Si ratio determined by XPS is about one tenth of the ratio for Ni/G[4]. This shows that a certain fraction of nickel is distributed in the small pores of G[4], probably resulting the high TOF value. It is supposed that small nickel particles are also present in the pores of Ni/G[4] although the major part of nickel is on the external surface. It can be evidenced by the significant reduction of the BET surface area of G[4] by impregnation of nickel, showing that a part of nickel particles being present in the pore choke the small pores. Hence, the presence of nickel particles in the small pore may cause the higher TOF value than with Ni/G[45]. In the case of Ni/SiO_2 the crystallite size of nickel seems to be close to the pore size, but the mean size of the pore in the bulk is estimated to be appreciably larger than the size of nickel particles, resulting in the lower TOF value than that for Ni/G[19].

References

[1] W. Keim (Ed.), Catalysis in C1 Chemistry, Reidel, Dordrecht, Holland, 1983.
[2] J.M. Fox III, Catal. Rev. Sci. Eng. 35 (1993) 169.
[3] National Research Council, Catalysis Looks to the Future, National Academy Press, Washington, D.C., 1992.
[4] M. Akiyoshi, H. Hattori, K. Tanabe, Sekiyu Gakkaishi 30 (1987) 156.
[5] A. Tada, Y. Watarai, K. Takahashi, Y. Imizu, H. Itoh, Chem. Lett. (1989) 543.
[6] J.Y. Ki, S.J. Kyeong, I.Y. Jae, J. Korean Inst. Chem. Eng. 31 (1993) 569.
[7] Y. Matsumura, N. Tode, T. Yazawa, M. Haruta, J. Mol. Catal. A 99 (1995) 183.
[8] L.H. Little, Infrared Spectra of Adsorbed Species, Academic Press, New York, 1966.
[9] E. Borello, A. Zecchina, C. Morterra, J. Phys. Chem. 71 (1967) 2938.
[10] E. Borello, A. Zecchina, C. Morterra, G. Ghiotti, J. Phys. Chem. 71 (1967) 2945.
[11] B.A. Morrow, J. Chem. Soc., Faraday Trans. 1 70 (1974) 1527.
[12] Y. Matsumura, K. Hashimoto, S. Yoshida, J. Catal. 117 (1989) 135.
[13] H. Tanaka, T. Yazawa, K. Eguchi, H. Nagasawa, N. Matsuda, T. Einishi, J. Non-Crystalline Solids 65 (1984) 301.
[14] H.P. Klug, L.E. Alexander, X-ray Diffraction Procedures, Wiley, New York, 1954.
[15] JCPDS file, 4-0850.
[16] D. Briggs, M.P. Seah (Eds.), Auger and X-ray photoelectron spectroscopy, in: Practical Surface Analysis, 2nd ed., vol. 1, Wiley, New York, 1990.
[17] J.W.E. Coenen, Appl. Catal. 75 (1991) 193.